

# Control Optimization for Parametric Hamiltonians by Pulse Reconstruction

Piero Luchi,\* Francesco Turro, Valentina Amitrano, and Francesco Pederiva

*Physics Department, University of Trento, Via Sommarive 14, I-38123 Trento, Italy and*

*INFN-TIFPA Trento Institute of Fundamental Physics and Applications, Via Sommarive, 14, I-38123 Trento, Italy*

Xian Wu, Kyle Wendt, Jonathan L Dubois, and Sofia Quaglioni

*Lawrence Livermore National Laboratory, P.O. Box 808, L-414, Livermore, California 94551, USA*

Optimal control techniques provide a means to tailor the control pulse sequence necessary for the generation of customized quantum gates, which help enhancing the resilience of quantum simulations to gate errors and device noise. However, the substantial amount of (classical) computing required for the generation of customized gates can quickly spoil the effectiveness of such an approach, especially when the pulse optimization needs to be iterated. We report the results of device-level quantum simulations of the unitary (real) time evolution of the hydrogen atom, based on superconducting qubit, and propose a method to reduce the computing time required for the generation of the control pulses. We use a simple interpolation scheme to accurately reconstruct the real time-propagator for a given time step starting from pulses obtained for a discrete set of pre-determined time intervals. We also explore an analogous treatment for the case in which the hydrogen atom Hamiltonian is parameterized by the mass of the electron. In both cases we obtain a reconstruction with very high fidelity and a substantial reduction of the computational effort.

## I. INTRODUCTION

The standard quantum computing (QC) approach, based on expressing arbitrary unitary operations in terms of a set of universal (or primitive) quantum gates, has been demonstrated to be in principle efficient for the simulation of complex systems on a quantum computer [1, 2]. In practice, the performance and reliability of the generated real-time evolution suffer from gate error rates and quantum device noise. In addition to extending the coherence time by improving the manufacturing process and the design of available qubits [3–5], a less explored route to improve the noise-resilience of quantum simulations consists in designing efficient quantum control protocols that allow the implementation of arbitrary quantum gates. This eliminates the need to split an arbitrary gate into its primitive constituents, obtaining both a shallower quantum circuit and a reduction in the noise that deep circuits produce. In particular, this work focuses on quantum optimal control [6, 7], defined as the procedure of designing microwave pulses that perform arbitrary unitary transformations using nonlinear optimization techniques. Rather than representing the unitary operator in terms of a set of predetermined ‘primitive’ gates, one tailors a control signal such that, applied at the same time to all the involved physical qubits, realizes the desired unitary transformation in one single application [8]. The quantum optimal control approach is very useful to simulate quantum mechanical systems where the standard approach performs poorly because of the need of very deep quantum circuits, with the consequence of generating large cumulative error rates [9]. However, it is not flawless. The optimization process

requires a substantial amount of computational power and time, which grows quickly with the dimensionality and complexity of the simulated system. Moreover, if the targeted unitary operator depends on some external or internal time-dependent parameter, the control signal needs to be recomputed at each simulation time-step. This drawback can be effectively addressed by finding a way to parametrize and reconstruct the control pulses, thereby avoiding a full re-evaluation for each realization of the time-dependent parameters. In this paper, we propose a method to reconstruct such control pulses for parametric Hamiltonians starting from a limited set of points in the parameter space using some simple fitting procedures. This protocol is applied and tested in the simulation of the 1s electron wavefunction of an Hydrogen atom, expanded in standard computational chemistry basis set, in two different contexts. The first is the reconstruction of the hydrogen atom propagation gate for a given time step from pre-evaluated pulses generating the real-time propagation over a discrete set of time intervals. The second is a simulation in which the Hamiltonian of the hydrogen atom depends parametrically on a time-varying effective mass of the electron,  $m_e$ . Once again, the signal providing the real-time propagator for a fixed time interval is evaluated for some arbitrary value of  $m_e$  starting from a finite set of controls. In the last section of this work, a slightly more complex reconstruction method, that makes use of Fourier transform and the interpolation is made on the set of spectra, is presented. This method will be able to deal with control pulses with a broad range of frequency components. In all cases, this reconstruction approach was able to obtain high-fidelity optimal control pulses with a reduced computational cost.

Quantum optimal control techniques are a very general tool and are, in principle, applicable to any hardware. In specifying the parameters for the optimization procedure,

---

\* [piero.luchi@unitn.it](mailto:piero.luchi@unitn.it)

one only has to take into account the specific characteristics of the quantum device. In this work we consider a multi-level superconducting circuit quantum electrodynamic (cQED) system [8, 10] given by a transmon [11, 12] coupled to the resonant mode of a microwave cavity. In particular, we adopt a three-dimensional transmon architecture [13]. Finally, the microwave control pulses driving the transmon were obtained with the optimization algorithm known as Gradient Ascent Pulse Engineering (GRAPE) [7, 14].

The structure of the present work is the following. Sec. II presents the details of the model studied and the mapping of the quantum states onto the  $N$ -levels superconducting circuit. A brief description of the adopted superconducting circuit and of the optimization algorithm can be found in Sec. III. A simple interpolation method for the reconstruction of the control pulses and the analysis of the corresponding results are described in Secs. IV and V, respectively. Finally Sec. VI presents the Fourier transform reconstruction method and conclusions are drawn in Sec. VII.

## II. HYDROGEN ATOM IN THE STO-KG BASIS

The s-wave Hydrogen atom in spherical coordinates is given by:

$$H_{hy} = \left[ -\frac{\hbar^2}{2m_e} \left( \frac{d^2}{dr^2} + \frac{2}{r} \frac{d}{dr} \right) - \frac{e^2}{r} \right], \quad (1)$$

where  $m_e$ ,  $\hbar$ , and  $e$  are, respectively, the electron mass, the reduced Planck constant and the electron charge, here used in the atomic units (and so, from now on, set to 1 unless otherwise specified). The ground state energy of this Hamiltonian is -0.5 Hartree.

In order to solve the Schrödinger equation describing the dynamics of the electron, we expand the electron orbital on a set of given basis functions, following the standard procedures used in computational chemistry [15]. There are two common choices for the basis function sets: The Slater type orbitals (STO), and the Gaussian type orbitals (GTO). STO have the general form:

$$B_{n,l,m,\zeta}(r, \theta, \phi) = NY_{l,m}(\theta, \phi)r^{n-1}e^{-\zeta r}, \quad (2)$$

while GTO have the form:

$$B_{n,l,m}(r, \theta, \phi) = NY_{l,m}(\theta, \phi)r^{2n-2-l}e^{-\zeta r^2}, \quad (3)$$

where  $N$  is a normalization constant,  $n, l, m$  are, respectively, the principal quantum number, the azimuthal quantum number and the magnetic quantum number and  $Y_{l,m}$  are spherical harmonics. In general, STO basis functions better represent the orbitals shape, having the correct asymptotic behaviour, but GTO are less computationally intensive. A compromise solution is to use a sum of  $K$  GTO function to approximate each STO function

i	$A_i$	$\alpha_i$
1	0.6789	0.1516
2	0.4301	0.8518

TABLE I: Values of  $A_i$  and  $\alpha_i$  for the  $1s$  orbital of the H atom (Eq. 5) in the STO-2G basis.

of a given basis, originating the STO-KG basis set. STO-KG orbitals have the following general form [16]:

$$B_{n,l,m,\zeta}(r, \theta, \phi) = Z(r, \theta, \phi) \sum_{i=1}^K A_i \left( \frac{2\alpha_i}{\pi} \right)^{\frac{3}{4}} e^{-\alpha_i r^2}, \quad (4)$$

where  $Z(r, \theta, \phi) = NY_{l,m}(\theta, \phi)r^{2n-2-l}$ ,  $K$  is the number of GTO functions used in the expansion and  $A_i$  and  $\alpha_i$  are numerical parameters obtained by a variational procedure [16]. Some of them are reported in Tab. I.

In general, atomic and molecular orbitals are represented by a sum of an adequate number of basis element in order to obtain a good approximation of the complete orbital and a good precision in the computation. For our investigation we only need to approximate the  $1s$  orbital so we need only one of this basis. We therefore set  $n = 1$  and  $l = m = 0$ , so that  $Y_{0,0}$  is constant and it can be neglected. Finally, the hydrogen wavefunction can be written as:

$$|\psi(r)\rangle = \sum_{i=1}^K A_i \left( \frac{2\alpha_i}{\pi} \right)^{\frac{3}{4}} e^{-\alpha_i r^2}. \quad (5)$$

In this work we limit ourselves to two GTO functions ( $K = 2$ ) in Sec. III and IV, where the general method is presented, and three GTO functions ( $K = 3$ ) in Sec. VI where a more complex example is showed. This allows for a one-to-one mapping between GTO basis functions and (Sofia) the levels of the 3D transmon.

## III. DEVICE HAMILTONIAN AND OPTIMIZATION PROCEDURE

To study the real-time propagation of the  $1s$  Hydrogen atom model described in Sec. II we follow the same procedure for the quantum simulation reported in Ref. [10], and expand the analysis by focusing on the parametrization of the control pulses.

A three-dimensional transmon coupled to a readout cavity can be described by the following Hamiltonian:

$$\hat{H}_d = \hbar\omega_T \hat{a}_T^\dagger \hat{a}_T + \hbar\omega_R \hat{a}_R^\dagger \hat{a}_R - E_J \left[ \cos(\hat{\phi}) + \frac{\hat{\phi}^2}{2} \right] \quad (6)$$

where  $\omega_T(\omega_R)$  is the bare frequency of the transmon (readout),  $\hat{a}_T$  and  $\hat{a}_T^\dagger$  ( $\hat{a}_R$  and  $\hat{a}_R^\dagger$ ) are the creation and annihilation operator for the transmon (readout),  $E_J$  is

the Josephson energy, and  $\hat{\phi}$  is the phase across the junction [17–19]. Following Ref. [10] we can rewrite Eq.(6) as:

$$\hat{H}_d = -\hbar \frac{\alpha_T}{2} \hat{a}_T^{\dagger 2} \hat{a}_T^2 - \hbar \frac{\alpha_R}{2} \hat{a}_R^{\dagger 2} \hat{a}_R^2 - \hbar \chi \hat{a}_T^\dagger \hat{a}_T \hat{a}_R^\dagger \hat{a}_R + O(\hat{\phi}^6) \quad (7)$$

with  $\alpha_{T(R)}$  the anharmonicity of the transmon (readout) and  $\chi$  the dissipative interaction between the transmon and the readout. Since the optimized control pulses must drive the transmon at about  $4\text{GHz}$  and hence the dominant frequency component of the control pulses will be about  $3\text{GHz}$  detuned from the readout cavity, we can safely neglect the term associated to the readout cavity. So the Hamiltonian of the system can be simplified to:

$$\hat{H}_d = -\hbar \frac{\alpha_T}{2} \hat{a}_T^{\dagger 2} \hat{a}_T^2 \quad (8)$$

where  $\alpha_T/2\pi = 2.1693\text{GHz}$

To implement a single time-step of the digital-time simulation, we apply a time-dependent drive which, in the frame of the transmon, can be expressed as a combination of an in-phase and in-quadrature pulse [20]:

$$\hat{H}_c = \hbar \epsilon_I(t) (\hat{a}_T^\dagger + \hat{a}_T) + i \hbar \epsilon_Q(t) (\hat{a}^\dagger - \hat{a}) \quad (9)$$

where  $\epsilon_{Q(I)}(t)$  is the real (imaginary) part of the time-dependent control. For a given digital-time step  $\Delta t$  we use the GRAPE algorithm to optimize the control sequences  $\epsilon_I(t)$  and  $\epsilon_Q(t)$  such that they satisfy, within a predetermined accuracy threshold, the equality:

$$\begin{aligned} U(\Delta t) &\equiv \exp \left( -\frac{i}{\hbar} \hat{H}_{hy} \Delta t \right) \simeq \\ &\simeq \mathcal{T} \exp \left\{ -\frac{i}{\hbar} \int_0^\tau \left[ \hat{H}_d + \hat{H}_c(\tau') \right] d\tau' \right\} \end{aligned} \quad (10)$$

where  $\mathcal{T} \exp \{ \}$  stands for a time-ordered exponential and  $\tau$  is the total duration of the control pulse. The left-hand side of equation (10) correspond to the short-time propagator we want to simulate, while the right-hand side is the propagator that is induced on the transmon by the control pulses  $\epsilon_{I(Q)}$ . Examples of optimal control pulses implementing the short-time propagation for the  $1s$  state of the Hydrogen atom expanded in STO-2G basis set, are presented in Fig. 1. Here are showed some control pulses corresponding to a set of  $\Delta t$  values. The analysis and the comment on this results are carried out in the Sec. V.

#### IV. CONTROL PULSE RECONSTRUCTION (CPR) METHOD

There are two main drawbacks in the use of algorithms such as GRAPE to compute optimized control sequences: the large computational cost and the general non-transferability of the generated optimized controls, meaning that any change in the unitary operator

requires a completely new computation. For instance, when studying the time evolution of a system, a new computation of the control pulses is required for each choice of the time step  $\Delta t$  in Eq. (10). The same holds if there is any parametric dependence of the Hamiltonian, and a study of the system is required as a function of the parameter value. One example is the simulation of a scattering process of two nucleons interacting through a spin/isospin dependent interaction, as captured by the leading order (LO) in the chiral effective field theory expansion. As described in Ref. [10] for the case of two neutrons, it is possible to break up the propagator in a spin-independent and a spin-dependent part, the latter being parametrically dependent on the instantaneous specific value of the coordinates of the neutrons. This implies that the control pulses implementing the instantaneous spin dynamics have to be computed at every time-step of the neutron's physical trajectory. This tends to neutralize the benefits in terms of computational speed-up that quantum computation allows in the simulation of quantum processes.

An explicit evaluation of the pulses for each value of the parameters can be avoided using the following general control pulse reconstruction (CPR) method. Given a Hamiltonian  $H(\Lambda)$ , where  $\Lambda = [\lambda_1, \lambda_2, \dots, \lambda_K]$ , is a point in the  $K$ -dimensional space of parameters characterizing the Hamiltonian, and assuming that one wants to implement on the quantum device the unitary transformation  $U(\Lambda) = \exp\{\{-i\Delta t H(\Lambda)\}\}$  making use of Eq. (10), one should:

1. Solve Eq. (10) (using GRAPE or some other equivalent optimization algorithm) for a discrete set of values of  $\Lambda$  and store the resulting control pulses. This allows to obtain a discrete set of controls each of which implements the specific unit transformation of a certain value of  $\Lambda$ .
2. Provide a fit of the pulses either in terms of a function (e.g. a polynomial fitting) or as an expansion over a basis (e.g. Fourier transform of the pulses). Let us call  $C = [c_1, c_2, \dots, c_M]$  the  $M$  coefficients of the fit (e.g. the polynomial coefficient or the spectra component).
3. Find a mathematical relationship  $C(\Lambda) = [c_1(\Lambda), c_2(\Lambda), \dots, c_M(\Lambda)]$  between the coefficients of the fit and the parameters of the unitary transformation  $U(\lambda_1, \dots, \lambda_K)$ . This will allow to obtain the  $c_i$  parameters given arbitrary  $\lambda_j$  values and therefore the control pulses that the  $c_i$  parameters identify.
4. Use this procedure to reconstruct the pulses for an arbitrary  $\Lambda$ . Select the  $\Lambda$  values of interest, recover the fit parameters through the mathematical relationship  $C(\Lambda)$ . These parameters can, finally, be used to reconstruct the control pulses.
5. Repeat point 4 in the simulation loop to recover all the needed control pulses.

## V. APPLICATION: SIMPLE PULSE FITTING PROCEDURE

In this section two simple kinds of simple parametric dependence of the Hydrogen short-time propagator will be presented. We expand the system Hamiltonian on the STO-2G basis and we use a single parameter dependence for the propagator, i.e.  $U(\Lambda) = U(\lambda_1)$ . We seek control pulse solutions of 50 ns in duration (well below the typical coherence time of superconducting qubits) with a sampling rate of 32 GHz (so the control is subdivided in  $N = 1600$  time-steps). We solve the optimization problem of Eq. (10) using the quantum toolbox in Python (QuTip) package [21]. Specifically, we employ the the GRAPE algorithm with the L-BFGS-B optimization method within the QuTip function `optimize_pulse_unitary`.

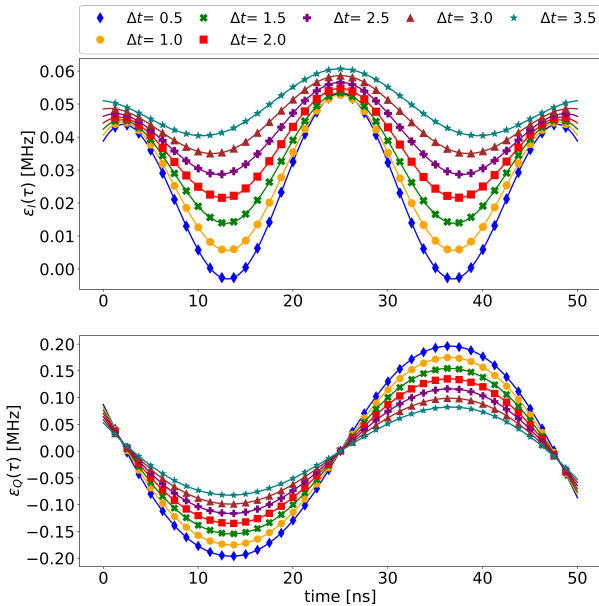


FIG. 1: Control pulses generating the short-time propagator for the 1s orbital of the Hydrogen atom expanded in the STO-2G basis set. Different curves correspond to different values of  $\Delta t$  as in Eq. (10). Upper panel:  $\epsilon_I$  (in-phase component of the signal). Lower panel:  $\epsilon_Q$  (in-quadrature component of the signal).

### A. Parameterization of the short-time propagator with $\Delta t$

In this first example, we choose as  $\Lambda$  the time-step of the short-time propagator for the Hydrogen atom introduced in Sec. II, i.e.  $\Lambda = \lambda_1 = \Delta t$ , namely:

$$U(\lambda_1) \equiv U(\Delta t) = e^{-i\Delta t H_{hy}}. \quad (11)$$

We start by calculating the control pulses corresponding to an equally spaced sequence of the parameter

$\Delta t_i = 0.5, 1.0, \dots, 3.5$  ns, with a required fidelity between the computed and target propagator of 99,9999%. The results are shown in Fig. 1. The initial guess for the first control pulses (for  $\Delta t_1 = 0.5$  Hartee $^{-1}$ ) is the zero function. After that, to ensure that the obtained pulses are a continuously varying family of functions, the initial guess for the control optimization at a given value of  $\Delta t_i$  is taken to be the solution for the previous parameter,  $\Delta t_{i-1}$ . In this way the solution of the optimization problem remains in the neighborhood of the same local minimum. Using the same (or a random) initial guess for different values of  $\Delta t_i$ , the solutions returned by the optimization algorithm can, in general, correspond to different local minima in the manifold of all the possible control pulses, giving rise to discontinuities that are undesirable for our present scope.

In a second step, the control pulses are fitted with a 10<sup>th</sup> degree polynomial, namely:

$$\epsilon_{Q(I)}(\tau; \Delta t) = \sum_{j=0}^{10} c_j \tau^j \quad (12)$$

where  $c_j = c_j(\Delta t_1, \dots, \Delta t_N) = c_j(\Delta t)$ . Fig. 2 shows the distribution of some of the coefficients  $c_j$  as a function of  $\Delta t$ . The  $c_0$  coefficient, which is the bias of the polynomial, and  $c_1$  depends almost linearly on  $\Delta t$ . In general,

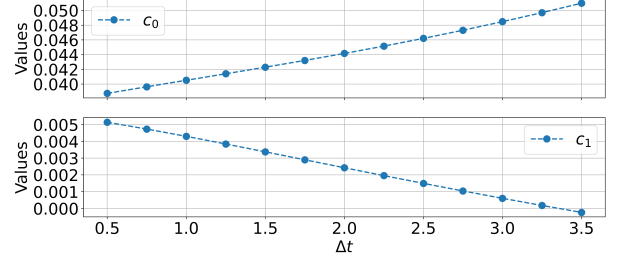


FIG. 2: Coefficients  $c_0$  and  $c_1$  of the polynomial fit (Eq. (12)) of the pulses in Fig. 1 as a function of the parameter  $\Delta t$ . In this case a linear relation might be safely assumed, but the dependence for other coefficients is not as simple and a 4<sup>th</sup> order polynomial was chosen to fit them (Eq. (13)).

we found that a 4<sup>th</sup> degree polynomial was sufficiently accurate to fit each  $c_i$  coefficient with respect to  $\Delta t$ . This polynomial can be written:

$$c_j(\Delta t) = \sum_{k=0}^4 b_k \Delta t^k, \quad (13)$$

where  $b_k$  are the polynomial coefficients. Referring again to Fig. 2, it can be seen that in both cases the  $c_j$  coefficients can be easily linked to the corresponding  $\Delta t$  value by the just introduced 4<sup>th</sup> degree polynomial (13).

Finally, we reconstruct the control pulse for an arbitrary value of  $\Delta t$  by using Eq. (13) to compute the corresponding coefficients, and evaluating the polynomial ex-

pression of Eq. (12) to obtain the reconstructed control pulses.

To test the validity of our reconstruction procedure, we used two distinct methods. First, we evaluate the fidelity  $\Phi$  of the short-time propagator computed from the reconstructed control pulses:

$$\Phi = \langle U_{ex} | U_{rec} \rangle \langle U_{rec} | U_t \rangle \quad (14)$$

where  $\langle U_{ex} | U_{rec} \rangle$  is the Hilbert-Schmidt inner product

$$\langle U_{ex} | U_{rec} \rangle = \frac{\text{Tr}\{U_{ex}^\dagger U_{rec}\}}{\dim(U_{ex})}, \quad (15)$$

$U_{ex}$  is the exact short-time propagator computed directly via Eq. (11), for  $\Delta t = \tilde{\Delta}t$  and  $U_{rec}$  is the short-time propagator computed from the reconstructed control pulses (for the same  $\tilde{\Delta}t$ ) using the right-hand-side of Eq. (10), as [14]. This provides a quantitative measure of the equivalence of the two unitary operators:  $\Phi$  is equal to 1 when the operators are equal and is equal to zero when they are completely uncorrelated. We found that the fidelity mean value is 0.99999998, almost equal to what one would obtain through standard control optimization procedure.

Second, we generated the control pulses for an arbitrary value of  $\Delta t$  (outside of the set used for the fitting) and checked that the corresponding real-time propagator  $U_{rec}(\tilde{\Delta}t)$  yields the desired quantum dynamics. Specifically, we considered  $\Delta t = 1.31 \text{ Hartee}^{-1}$ . The reconstruction procedure provides the pulses plotted in Fig. 3 together with the original set of pulses used in the fitting procedure. As expected, the new control pulses lay in between the solutions for  $\Delta t$  values greater and smaller than  $1.31 \text{ Hartee}^{-1}$ .

Using the real-time propagator for the Hydrogen atom,  $U_{rec}(\Delta t) = 1.31 \text{ Hartee}^{-1}$ , we then implement a (classical computing) simulation of the quantum system starting from an arbitrary initial condition. We then compare the results with the exact system evolution obtained through a direct numerical solution of the time-dependent Schrödinger equation. Figure 4 visualizes such comparison as well as a second example obtained for a different value of  $\Delta t$ . The simulated quantum gate propagation (represented by dots) follow closely the exact time evolution of the system (solid lines) computed from the direct solution of the time dependent Schrödinger equation.

## B. Parametrization of the Hamiltonian with the effective mass

In this second example we select the  $\Lambda$  parameter to be the mass of the electron  $m_e$ , (see Eq. (1)) so the dependence can be written explicitly as:

$$U(\lambda) \equiv U(m_e) = e^{-i\Delta t H_{hy}(m_e)}. \quad (16)$$

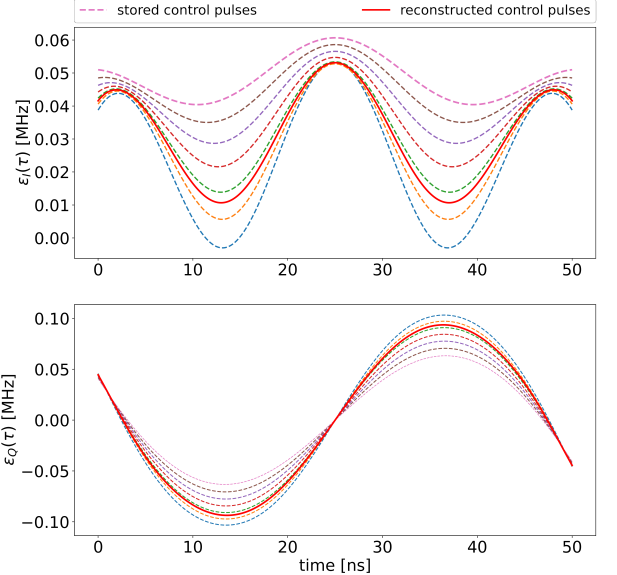


FIG. 3: Reconstructed control pulse (red solid line) for  $\Delta t = 1.31 \text{ Hartee}^{-1}$ . The reconstructed control lies in between controls for  $\Delta t$  greater and smaller than  $1.31$ . *Upper panel:* In-Phase components  $\epsilon_I(t)$ . *Lower panel:* In-Quadrature components  $\epsilon_Q(t)$

Since we are using atomic units,  $m_e$  is equal to 1 and, as a parameter, it will be varied around 1 for the pulse computation. This example has no real physical meaning but it is very instructive and useful to test the CPR method on a non trivial parameter dependence. A generalization of this Hamiltonian might describe the dynamics of an electron in a crystal in presence of a Berry's curvature due to an external magnetic field [22].

The procedure employed to study exactly follows the one reported in the previous subsection. We begin by computing the control pulses for an equally spaced sequence of mass values  $m_e = 0.7, 0.8, \dots, 1.9$ , and then fit the controls with a 6<sup>th</sup> degree general polynomial. Results are shown in Fig. 5. Once again, computing the control pulses with GRAPE we find a slowly varying family of them. This reassures us that our method can be applied also in this more general and non-trivial case.

Also in this case the reconstruction procedure works well, yielding a mean fidelity of 0.999997.

Since the aim of this work is to find a method to enhance the performance of a simulation in which the short-time propagator parameters are, in turn, dependent on time, we set up a calculation in which at every time-step the mass is changed according to the equation:  $m_e^j = 1.0 + 0.2 \sin(j\pi/N_{\max})$  for  $j = \{0, 1, \dots, N_{\max}\}$ . So we proceed, iteratively, by changing the mass, reconstructing the controls with CPR method, computing the propagator and then applying it to advance the simulation. The results are presented in Fig. 6. We see that the approximate evolution obtained by this method, follows very closely the exact evolution. An estimate of the

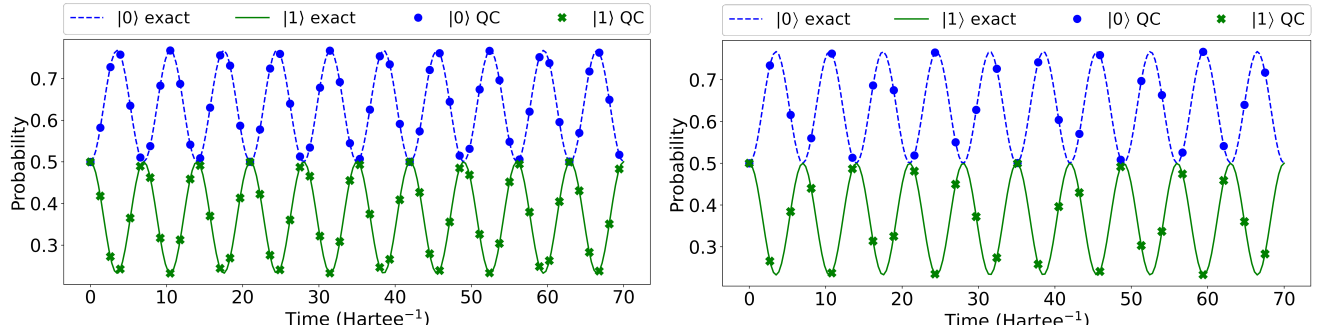


FIG. 4: Temporal evolution of the Hydrogen system expandend on STO-2G basis. *Left*: Comparison between the exact evolution (solid line) and dynamics obtained through the repeated application of the short-time propagator computed from the reconstructed controls (dots) for  $\Delta t = 1.31$  Hartee $^{-1}$ . *Right*: Another example of temporal evolution with  $\Delta t = 2.70$  Hartee $^{-1}$ . Note that in both cases an arbitrary  $\Delta t$  was used and the dynamics follows closely the exact one obtained from the numerical resolution of Schrödinger Eqaution

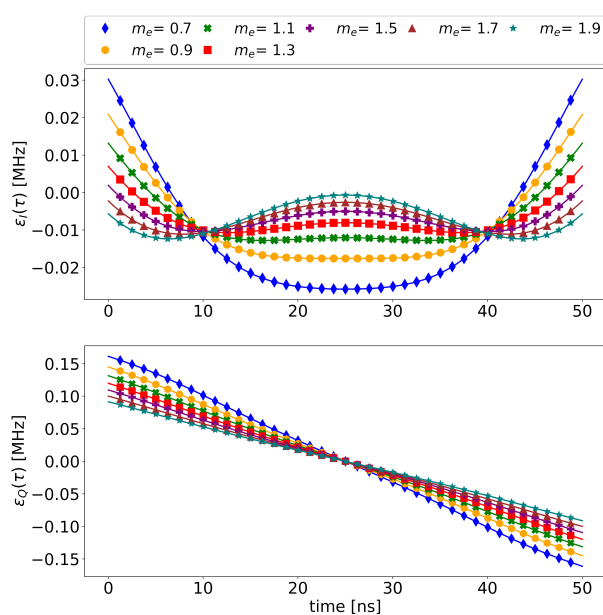


FIG. 5: In-phase component (upper plot) and In-quadrature component (lower plot) of control pulses for different values of the electron mass  $m_e$  (in atomic units).

gain in performance can be obtained by comparing the computing time needed to produce a step with our RPC method and with the standard optimization procedure. On average one step with our fitting method takes 2.48 seconds, while using GRAPE it takes on average 31.12 seconds. The ratio between these times is 12.47, which means that the proposed method is, on average, 12 times faster (in the device level simulation framework).

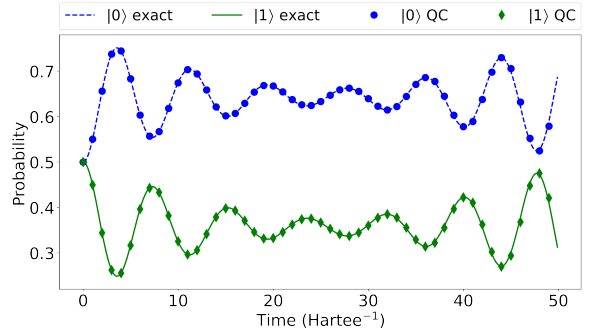


FIG. 6: Temporal evolution of the Hydrogen atom system for for cyclic variation of the electron mass  $m_e$ . At every time-step the control pulses are reconstructed via CPR Method and used to advance the simulation. The propagator obtained through the reconstructed controls (dots) follows closely the exact evolution (solid line).

## VI. CONTROL PULSE RECONSTRUCTION VIA FOURIER TRANSFORM (CPRFT) METHOD

So far we have considered cases for which the driving pulses resulting from the optimization procedure are rather simple, and can be directly fitted with an ad-hoc functional form. However, in general, the pulses have shapes that cannot be easily interpreted in terms of elementary functions, since they could contain multiple frequency components. A possible solution is to use an expansion over a set of basis set. In the general scheme presented in Sec. IV, the step of fitting the pulse is then simply replaced by finding the expansion coefficients over the chosen basis. For periodic signals an obvious choice is that of operating a Fourier transform on each of the pulses  $\epsilon_{Q(I)}(t, \Lambda)$ . The resulting set of curves  $\tilde{\epsilon}_{Q(I)}(\omega, C)$ , which are in turns the spectra of the control pulses, needs then to be interpolated as a function of  $\Lambda = \lambda = m_e$ , in-

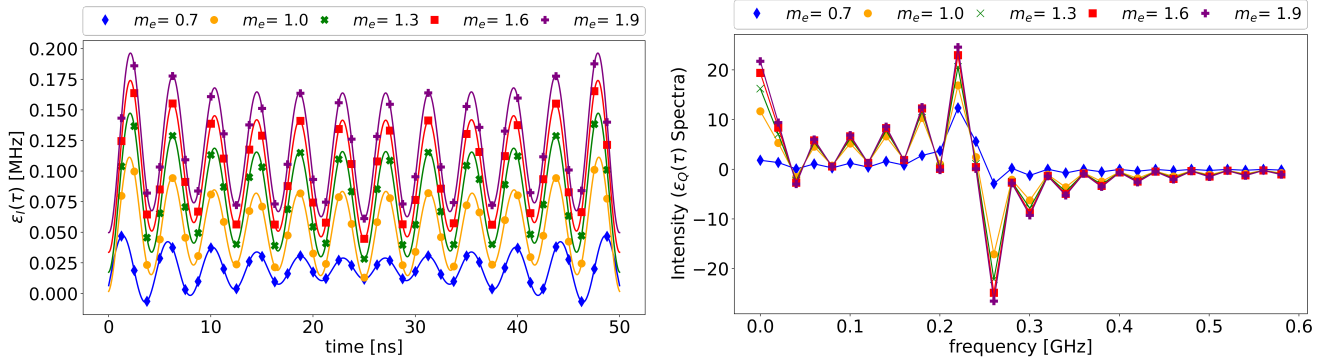


FIG. 7: Left: The real part of control pulses for the 3 level hydrogen atom. The pulses implement a time propagator  $U(m_e)$  for the set of values of  $m_e$  reported in the legend. Right: Spectra of the control pulses of the 3 level hydrogen atom coming from the Fourier transform of the control pulses

terpreting each frequency of the spectra as a component  $c_j$  of the coefficient vector  $C$ . A driving pulse for an arbitrary point in the parameter space can then be obtained by interpolating the corresponding spectrum and back Fourier transforming it.

We worked out an application of this method to the electron-mass dependent Hydrogen atom. In order to have a less trivial control pulse, we expanded the Hydrogen Hamiltonian on a STO-3G basis set and then mapped the states of the system onto a 3 level transmon. The Hamiltonian is now given by a  $3 \times 3$  matrix.

In Fig. 7,  $\epsilon_Q(t, m_e)$  control pulses for the 3 level system are presented. It can be seen that the controls present higher frequencies components and the fitting method described in the previous sections would be of no use. However, also in this case one can still notice that a smoothly varying family of controls emerges.

Now, we Fourier transform the control pulses, obtaining a set of spectra, plotted in the right panel of Fig. 7. Each frequency of the spectrum changes smoothly as a function of the electron mass  $m_e$ . Hence, we can interpolate each component of the spectrum and reconstruct it for an arbitrary value of  $m_e$ . Once we obtain the new spectrum we can transform it back to the time domain, obtaining finally the reconstructed control pulse.

These control pulses can now be used to directly implement a gate in the real transmon setup or, in the case of our simulation, to reconstruct the propagator used to test the method.

We reconstructed the control pulse for  $m_e = 1.45$ , and then evolved the system starting from an arbitrary initial state, as can be seen in Fig. 8.

The agreement between the exact solution and the solution provided by the Control Pulse Reconstruction via Fourier Transform (CPRFT) method here presented is excellent. The mean fidelity for a fine grid of  $m_e$  values is 0.99998. Although the addition of the third level and the use of a transform on the pulses lower the mean fidelity of the CPRFT method, its value is still at an acceptable level, also considering the computational speed-up.

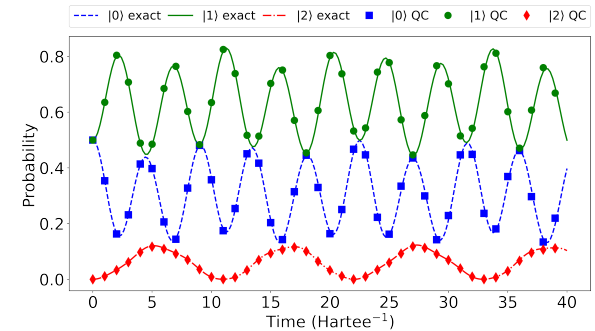


FIG. 8: Test of the accuracy of the Fourier transform method as it would be applied on a 3-states transmon. For  $m_e = 1.45$ , an arbitrary initial state is evolved both using the reconstructed propagator (dots) and directly solving the time dependent Schrödinger equation (solid lines). The agreement is very good.

Furthermore it allows good simulation results, as already showed in Fig. 8.

## VII. CONCLUSION

We introduced a general scheme, the Control Pulse Reconstruction (CPR) method, that can be used to increase the performance of quantum computations based on optimal control techniques whenever a frequent evaluation of the control pulses is needed. In general this corresponds to consider a family of Hamiltonians or propagators that are dependent by some parameter, which is turn a function of the evolution time. As a test of this protocol, we presented the simulation of the real time evolution of the electron wave function of the hydrogen atom mapped on a controllable multi-level superconducting quantum computer. The  $1s$  state of the H atom was expanded in the STO-2G basis. The control pulses for the single multi-level gate, necessary to encode the propagator onto

the quantum device, was obtained by a numerical optimization using the GRAPE algorithm as implemented in the QuTiP python package. By calculating a set of control pulses of propagators which differ in the value of a parameter and, then, finding a functional dependence between the shape of these control pulses, it was possible to derive a mathematical model that allows to reconstruct the control pulses of an arbitrary value bypassing the numerical optimization. We showed results for two realization of this procedure. A first simple one makes use of polynomial fitting. A more complex one uses instead the CPRFT method meant to interpolate periodic pulses of arbitrary shape. To investigate the performance of our approach we compared evolution of the reconstructed propagator with the exact evolution of the system, and, furthermore, computed the fidelity between the exact and the reconstructed propagator, obtaining in all cases excellent results. We also presented a simulation of the hydrogen Hamiltonian with a time-dependent electron effective mass, for which we showed that the time required to perform the simulation with our method is one order of magnitude smaller than the original approach.

Complex systems whose Hamiltonian depends on some external parameters require the control pulses to be optimized at every time-step. So this method, avoiding the great amount of time and computational resources needed for the computation, could be of great interest to improve the quantum systems simulation of realistic systems. More complex situations, as the study of nucleon spin dynamics, could indeed strongly benefit of this method. In particular, it opens the possibility for a manageable implementation of several classical-quantum co-processing protocols.

## VIII. ACKNOWLEDGMENT

This research was partially supported by Q@TN grants ML-QForge (PL) and ANuPC-QS (FT). This work was prepared in part by LLNL under Contract DE-AC52-07NA27344 with support from the Laboratory Directed Research and Development grant 19-DR-005.

---

[1] D. P. DiVincenzo, *Fortschritte der Physik: Progress of Physics* **48**, 771 (2000).

[2] R. Barends, L. Lamata, J. Kelly, L. García-Álvarez, A. Fowler, A. Megrant, E. Jeffrey, T. White, D. Sank, J. Mutus, *et al.*, *Nature communications* **6**, 1 (2015).

[3] A. P. Place, L. V. Rodgers, P. Mundada, B. M. Smitham, M. Fitzpatrick, Z. Leng, A. Premkumar, J. Bryon, S. Sussman, G. Cheng, *et al.*, arXiv preprint arXiv:2003.00024 (2020).

[4] A. Nersisyan, S. Poletto, N. Alidoust, R. Manenti, R. Renzas, C.-V. Bui, K. Vu, T. Whyland, Y. Mohan, E. A. Sete, *et al.*, (2019).

[5] L. B. Nguyen, Y.-H. Lin, A. Somoroff, R. Mencia, N. Grabon, and V. E. Manucharyan, *Physical Review X* **9**, 041041 (2019).

[6] J. Werschnik and E. Gross, *Journal of Physics B: Atomic, Molecular and Optical Physics* **40**, R175 (2007).

[7] N. Khaneja, T. Reiss, C. Kehlet, T. Schulte-Herbrüggen, and S. J. Glaser, *Journal of magnetic resonance* **172**, 296 (2005).

[8] X. Wu, S. Tomarken, N. A. Petersson, L. Martinez, Y. J. Rosen, and J. L. DuBois, *Physical Review Letters* **125**, 170502 (2020).

[9] P. J. O’Malley, R. Babbush, I. D. Kivlichan, J. Romero, J. R. McClean, R. Barends, J. Kelly, P. Roushan, A. Tranter, N. Ding, *et al.*, *Physical Review X* **6**, 031007 (2016).

[10] E. T. Holland, K. A. Wendt, K. Kravvaris, X. Wu, W. E. Ormand, J. L. DuBois, S. Quaglioni, and F. Pederiva, *Physical Review A* **101**, 062307 (2020).

[11] H. Paik, D. Schuster, L. S. Bishop, G. Kirchmair, G. Catelani, A. Sears, B. Johnson, M. Reagor, L. Frunzio, L. Glazman, *et al.*, *Physical Review Letters* **107**, 240501 (2011).

[12] J. Koch, M. Y. Terri, J. Gambetta, A. A. Houck, D. Schuster, J. Majer, A. Blais, M. H. Devoret, S. M. Girvin, and R. J. Schoelkopf, *Physical Review A* **76**, 042319 (2007).

[13] M. Kjaergaard, M. E. Schwartz, J. Braumüller, P. Krantz, J. I.-J. Wang, S. Gustavsson, and W. D. Oliver, *Annual Review of Condensed Matter Physics* **11** (2019).

[14] B. Rowland and J. A. Jones, *Philosophical Transactions of the Royal Society A: Mathematical, Physical and Engineering Sciences* **370**, 4636 (2012).

[15] F. Jensen, *Introduction to computational chemistry* (John Wiley & Sons, 2017).

[16] W. J. Hehre, R. F. Stewart, and J. A. Pople, *The Journal of Chemical Physics* **51**, 2657 (1969).

[17] S. E. Nigg, H. Paik, B. Vlastakis, G. Kirchmair, S. Shankar, L. Frunzio, M. Devoret, R. Schoelkopf, and S. Girvin, *Physical Review Letters* **108**, 240502 (2012).

[18] P. Krantz, M. Kjaergaard, F. Yan, T. P. Orlando, S. Gustavsson, and W. D. Oliver, *Applied Physics Reviews* **6**, 021318 (2019).

[19] A. Blais, R.-S. Huang, A. Wallraff, S. M. Girvin, and R. J. Schoelkopf, *Physical Review A* **69**, 062320 (2004).

[20] R. W. Heeres, P. Reinhold, N. Ofek, L. Frunzio, L. Jiang, M. H. Devoret, and R. J. Schoelkopf, *Nature communications* **8**, 1 (2017).

[21] .

[22] M. J. Rave and W. C. Kerr, *European Journal of Physics* **31**, 15 (2010).